General and Comparative Endocrinology 340 (2023) 114304

Contents lists available at ScienceDirect

General and Comparative Endocrinology

journal homepage: www.elsevier.com/locate/ygcen

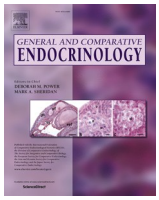

Effects of molting on the expression of ecdysteroid biosynthesis genes in the Y-organ of the blackback land crab, *Gecarcinus lateralis*

Samiha A.M. Benrabaa [a], Sharon A. Chang [b], Ernest S. Chang [b], Donald L. Mykles [a,b,*]

[a] Colorado State University, Fort Collins, CO 80523, USA
[b] Bodega Marine Laboratory, University of California, Davis, Bodega Bay, CA 94923, USA

ARTICLE INFO

Keywords:
Ecdysteroid
Halloween gene
Cytochrome P450
Y-organ
Molting

ABSTRACT

A pair of Y-organs (YOs) synthesize ecdysteroids that initiate and coordinate molting processes in decapod crustaceans. The YO converts cholesterol to secreted products through a biosynthetic pathway involving a Rieske oxygenase encoded by *Neverland* (*Nvd*) and cytochrome P450 monooxygenases encoded by Halloween genes *Spook* (*Spo*; *Cyp307a1*), *Phantom* (*Phm*; *Cyp306a1*), *Disembodied* (*Dib*; *Cyp302a1*), and *Shadow* (*Sad*; *Cyp315a1*). NAD kinase (NADK) and 5-aminolevulinic acid synthase (ALAS) support ecdysteroid synthesis in insects. A 20-hydroxylase, encoded by *Shed* in decapods and *Shade* in insects, converts ecdysone to the active hormone 20-hydroxyecdysone (20E). 20E is inactivated by cytochrome P450 26-hydroxylase (Cyp18a1). Contigs encoding these eight proteins were extracted from a *Gecarcinus lateralis* YO transcriptome and their expression was quantified by quantitative polymerase chain reaction. mRNA levels of *Gl-Spo* and *Gl-Phm* were four orders of magnitude higher in YO than those in nine other tissues, while mRNA levels of *Gl-NADK* and *Gl-ALAS* were similar in all ten tissues. In *G. lateralis* induced to molt by multiple leg autotomy, YO mRNA levels of *Gl-Nvd*, *Gl-Spo*, *Gl-Phm*, *Gl-NADK*, and *Gl-ALAS* were highest in intermolt and premolt stages and lower in postmolt. *Gl-Dib* mRNA level was not affected by molt stage. mRNA level of *Gl-Sad*, which converts 2-deoxyecdysone to ecdysone, was higher in mid- and late premolt stages, when YO ecdysteroidogenic capacity is greatest. *Gl-Cyp18a1* mRNA level was highest in intermolt, decreased in premolt stages, and was lowest in postmolt. In animals induced to molt by eyestalk ablation, YO mRNA levels of all eight genes were not correlated with increased hemolymph 20E titers. These results suggest that YO ecdysteroidogenic genes are differentially regulated at transcriptional and translational levels.

1. Introduction

Ecdysteroid hormones control molting in arthropods. Steroidogenic organs, such as the prothoracic gland in insects and the Y-organ (YO) in decapod crustaceans, convert cholesterol obtained from the diet to ecdysteroids (Kamiyama and Niwa, 2022; Kannangara et al., 2021; Mykles, 2011; Pan et al., 2021). The ecdysteroid biosynthetic pathway is similar between insects and crustaceans (Lafont et al., 2012; Mykles, 2011). Cholesterol is converted to 7-dehydrocholesterol (7DC) by a 7,8-dehydrogenase encoded by *Neverland* (*Nvd*) (Yoshiyama-Yanagawa et al., 2011). "Black box" enzymes, such as Shroud (Sro; CYP6T3) and Spook (Spo; CYP307a1), and a 5β [H]-reductase convert 7DC to 5β-diketol. 5 β -Diketol is converted to 5 β -ketodiol by 3-dehydroecdysteroid-3 β -reductase (Mykles, 2011; Niwa and Niwa, 2014). Cytochrome P450 enzymes encoded by Halloween genes *Phantom* (*Phm*; *CYP306a1*), *Disembodied* (*Dib*; *CYP302a1*), and *Shadow* (*Sad*; *CYP315a1*) hydroxylate 5β-ketodiol at C25, C22, and C2, respectively, to ecdysone (Gilbert and Rewitz, 2009; Mykles, 2011; Niwa and Niwa, 2014). Unlike insects, in which ecdysone is the primary product of the prothoracic gland, the crustacean YO can secrete ecdysone, 25-hydroxyecdysone, 3-dehydroecdysone, and 3-dehydro-25-deoxyecdysone (Mykles, 2011). A 20-hydroxylase (Cyp314a1) encoded by *Shade* (*Shd*) in insects and *Shed* in decapod crustaceans converts ecdysone and 25-deoxyecdysone to the active hormones 20-hydroxyecdysone (20E) and ponasterone A (PA), respectively (Mykles, 2011; Swall et al., 2021; Ventura et al., 2017, 2018). A 26-hydroxylase, encoded by *Cyp18a1*, inactivates 20E and PA and leads to their degradation and elimination (Dermauw et al., 2020; Guittard et al., 2011; Mykles, 2011).

Arthropod cytochrome P450 enzymes belong to a gene superfamily of heme-thiolate proteins that are organized into six CYP clans,

* Corresponding author at: Department of Biology, Colorado State University, Fort Collins, CO 80523, USA.
E-mail address: donald.mykles@colostate.edu (D.L. Mykles).

https://doi.org/10.1016/j.ygcen.2023.114304
Received 14 February 2023; Received in revised form 24 March 2023; Accepted 28 April 2023
Available online 29 April 2023

designated mitochondrial, CYP2, CYP3, CYP4, CYP16, and CYP20 (Dermauw et al., 2020). Halloween genes and *Cyp18a1* are grouped into the CYP2 (*Spo* and *Phm*) and mitochondrial (*Dib*, *Sad*, *Shd/Shed*, and *Cyp18a1*) clans (Dermauw et al., 2020; Feyereisen, 2012; Guittard et al., 2011). Spo and Phm are microsomal proteins associated with the endoplasmic reticulum, whereas Dib, Sad, Shd/Shed, and Cyp18a1 are located in mitochondria (Feyereisen, 2012). Ecdysteroidogenic enzymes are characterized by a heme-binding domain containing a PFxxGxRxCxG/A consensus sequence, in which the cysteine interacts with the heme iron (Feyereisen, 2012; Gilbert and Rewitz, 2009; Xie et al., 2016). Other conserved sequences are Helix-C (GxxWxEQRR), Helix-I (GxE/DTT/S), Helix-K (ExLR), and PERF (PxxFxPE/DRF) (Asazuma et al., 2009; Dermauw et al., 2020; Feyereisen, 2012; Gilbert and Rewitz, 2009; Swall et al., 2021; Xie et al., 2016). The N-terminal region of microsomal P450 (e.g., Spo and Phm) is characterized by a hydrophobic segment followed by a proline/glycine (P/G) rich domain (Asazuma et al., 2009; Iga and Smagghe, 2010; Swall et al., 2021; Xie et al., 2016).

Molt-inhibiting hormone (MIH), a neuropeptide released from the X-organ/sinus gland complex in the eyestalk ganglia, controls molting through inhibition of the YOs (Hopkins, 2012; Mykles and Chang, 2020). The YO progresses through four phenotypic states that are associated with molt cycle stages: basal state during intermolt (stage C_4); activated state during early premolt (stage D_0); committed state during mid- and late premolt (stages D_1 and D_2, respectively); and repressed state during postmolt (stages A, B, and $C_{1\text{-}3}$) (Mykles and Chang, 2020). Molting is initiated when a decrease in MIH release activates the YOs, which hypertrophy and increase ecdysteroid production in early premolt (Mykles and Chang, 2020). A downstream target of MIH signaling, which involves a cAMP/Ca^{2+}-dependent triggering phase and an NO/cGMP-dependent summation phase, is mechanistic Target of Rapamycin Complex 1 (mTORC1) (Covi et al., 2009; Mykles and Chang, 2020). mTORC1 is a rapamycin-sensitive protein kinase complex that controls protein translation, lipid and nucleotide synthesis, autophagy, and lysosome biosynthesis (Battaglioni et al., 2022; Melick and Jewell, 2020; Saxton and Sabatini, 2017). Rapamycin inhibits YO ecdysteroidogenesis *in vitro* in *Gecarcinus lateralis* and *Carcinus maenas* and blocks molt initiation *in vivo* in *G. lateralis* (Abuhagr et al., 2014b; Abuhagr et al., 2016). In *G. lateralis*, *Gl-mTOR* expression increases during premolt (Abuhagr et al., 2016). In *Eriocheir sinensis*, RNAi knockdown of *Es-mTOR* lengthens the molt interval 16%, from 34 days to 39.3 days (Hou et al., 2021). The activity of mTORC1 is controlled by the small GTPase Ras homolog enriched in brain (Rheb). Active GTP/Rheb stimulates mTORC1 activity (Melick and Jewell, 2020). The tuberous sclerosis complex (TSC), a GTPase-activating protein, inactivates Rheb by promoting the hydrolysis of GTP to GDP. It is hypothesized that cGMP-dependent protein kinase (PKG) inhibits mTORC1 via TSC and Rheb (Mykles, 2021). These data suggest that YO activation requires mTORC1-dependent protein synthesis by initially stimulating translation of mRNAs, followed by altering the expression of thousands of genes that drive the transition of the YO from the activated to committed state (Das et al., 2018; Mykles, 2021; Shyamal et al., 2018).

Transcriptomics has identified contigs encoding ecdysteroid biosynthetic and degradative pathway genes in the YO of *G. lateralis* (Shyamal et al., 2018; Swall et al., 2021) and other decapod species (Andersen et al., 2022; Legrand et al., 2021; Tom et al., 2013; Ventura et al., 2017; Wang et al., 2020). cDNAs encoding Halloween genes *Nvd*, *Phm*, *Sad*, and *Spo* have been characterized (Asazuma et al., 2009; Sathapondecha et al., 2017; Xie et al., 2016). This study characterized eight genes involved in ecdysteroid metabolism that are expressed in the *G. lateralis* YO. *Gl Nvd*, *Gl-Spo*, *Gl-Phm*, *Gl-Dib*, and *Gl-Sad* encode enzymes in the ecdysteroidogenic pathway and *Gl-Cyp18a1* encodes a 26-hydroxylase (Mykles, 2011). A cytochrome P450 20-monooxygenase encoded by six *Gl-Shed* contigs was previously characterized (Swall et al., 2021). NAD kinase (NADK) and 5-aminolevulinic acid synthase (ALAS) catalyze reactions for NADP(H) production and heme biosynthesis, respectively (de Mena et al., 1999; Lerner et al., 2001; Love et al., 2015; Ohashi et al., 2012; Okano et al., 2010). Contigs encoding *Gl-ALAS*, and *Gl-NADK*, which support ecdysteroidogenesis in the insect prothoracic gland (Nakaoka et al., 2017), were also characterized. Quantitative polymerase chain reaction (qPCR) was used to quantify mRNA levels in ten tissues from intermolt animals and in the YO from animals induced to molt by multiple leg autotomy (MLA) or by acute withdrawal of MIH by eyestalk ablation (ESA).

2. Materials and methods

2.1. Animals and experimental treatments

Adult male *Gecarcinus lateralis* were shipped from the Dominican Republic and maintained at Colorado State University (Swall et al., 2021). Molting was induced by autotomy of 8 walking legs (MLA) or by ESA (Mykles and Chang, 2020). Premolt stages were monitored by limb bud growth, as measured by the regeneration (R) index (Yu et al., 2002). Hemolymph ecdysteroid titers were quantified by a competitive enzyme-linked immunosorbant assay (ELISA) (Abuhagr et al., 2014a).

2.2. Characterization of contig sequences in the YO transcriptome

A custom tBLASTn web portal was used in the running a BLAST search with each of the eight protein sequences derived from NCBI against the *G. lateralis* YO transcriptome (Das et al., 2018; Swall et al., 2021). The full nucleotide sequences of the selected contigs were obtained for all 8 genes from the transcriptome using prfectBlast (Santiago-Sotelo and Ramirez-Prado, 2012). Protein sequences were obtained using the online ExPASy translate tool (Artimo et al., 2012). The Swiss Institute of Bioinformatics was used to identify the open reading frame (ORF) for each of the contigs that were extracted, selecting the longest ORF that matched the reading frame that the transcriptome tBLASTn returned. The sequences of *Gl-Phm*, *Gl-Sad*, *Gl-Spo*, and *Gl-Nvl* were confirmed by direct sequencing of PCR products from YO cDNA using sequence-specific primers (Suppl. Table 1). The sequences of all eight contigs were deposited in GenBank and their accession numbers are given in Table 2 and Supplementary Data 1.

Multiple alignments of amino acid sequences identified conserved regions and motifs. Clustal X version 2.1 (Larkin et al., 2007) and GeneDoc version 2.7 (Nicholas et al., 1997) were used to generate and edit sequence alignments. The Conserved Domain Database was used to identify the variable regions in each gene and the results were cross-referenced with published information on the structure of each gene in other species (Marchler-Bauer et al., 2015).

For phylogenic analysis, multiple protein sequence alignments produced by ClustalW2 software was used to generate phylogenetic trees using UGENE software (Okonechnikov et al., 2012; Thompson et al., 1994). Interactive Tree of Life (iTOL) and Maximum Likehood Tree software were used to display the phylogenic trees (http://itol.embl.de) (Letunic and Bork, 2016).

2.3. Quantification of tissue mRNA levels

RNA isolation, DNase treatment, and cDNA synthesis are described (Swall et al., 2021). RNA was quantified by absorbance at 260 nm with a NanoDrop ND-1000 (Abuhagr et al., 2014a). qPCR was performed on a Light cycler 480 Thermocycler (Roche Applied Science, Indianapolis, IN, USA). Reactions contained 0.5 μl each of forward and reverse gene-specific primers (Table 1), 5 μl SYBR Green (Roche), 3 μl nuclease free water, and 1 μl cDNA. Reaction conditions were: denaturation for 3 min at 95 °C; 45 cycles, each cycle consisting of 30 sec at 95 °C, 30 sec at 62 °C, and 20 sec at 72 °C; and a final extension of 7 min at 72 °C. The data are expressed as log copy number per μg total RNA (mean ± 1 S.E., n = sample size).

Table 1
Oligonucleotide primers used for quantitative PCR of *G. lateralis* ecdysteroid metabolism genes. Abbreviations: bp, base pairs; F, forward; R, reverse; and TM, annealing temperature.

Gene	Primer Sequence (5′–3′)	Product size (bp)	TM (C)
Phantom	F1: TCTTTCACTTCACCACCACC	182	54.9
	R1: TCCTCTGTGACTCAGGTCTTA		54.4
Disembodied	F1: TCTCTTCAGTCAGTCCCTATGT	234	54.6
	R1: GCATCTCAGCTACCTCTCATTT		54.6
Shadow	F1: CGGCTGACTCCCTCATAATTT	234	54.7
	R1: GGAAGGCAGCTCGCTATAAG		55.4
Spook	F1: CCCTTCAGCACCGGAAAG	251	56.2
	R1: CTAGTGATACTCGTGATGCCTG		54.6
Neverland	F1: GTGTCCGAGGCGAGACATT	183	57.3
	R1: ACGTCGACCATCACCATTAC		54.7
CYP18a1	F1: CACTGTCATTCCACTCCTCTAC	177	54.6
	R1: TCACTCCTCGCCAAGACATT		56.2
ALAS	F1: CAAGGTCTCGGATGAACTGATAA	129	54.3
	R1: CATACCAAGCCCATGATGGA		54.7
NADK	F1: GCCGAATCATGCGAAACTC	101	54.5
	R1: CTTGTCTGTGTTGGTCATCAAG		53.9

2.4. Statistical analysis and graphing

SigmaPlot (Systat Software, Inc.) was used for statistical analysis and graphing. One-way ANOVA and Tukey *post-hoc* tests were used to determine differences in mean values between groups ($p < 0.05$). A Dunn's *post-hoc* test was used if equal variance tests failed ($p < 0.05$).

3. Results

3.1. Ecdysteroid metabolism genes in G. lateralis YO transcriptome.

Eight contiguous sequences encoding proteins involved in ecdysteroid metabolism were extracted from a *G. lateralis* YO transcriptome (Table 2). The transcriptome was assembled from high-throughput RNA sequencing (RNA-seq) of YOs from animals at intermolt, early premolt, mid-premolt, late premolt, and 10-day postmolt stages (Das et al., 2018). Full-length contigs encoding a Rieske oxygenase enzyme (*Gl-Nvd*), five cytochrome P450 enzymes (*Gl-Phm*, *Gl-Dib*, *Gl-Sad*, *Gl-Spo*, and *Gl-CYP18a1*), a NAD kinase (*Gl-NADK*), and a 5-aminolevulinic acid synthase (*Gl-ALAS*) were obtained (Suppl. Data 1). The sequences of *Gl-Phm*, *Gl-Sad*, *Gl-Spo*, and *Gl-Nvd* were confirmed by direct sequencing of PCR products amplified from YO cDNA (see Materials and Methods; data not shown). Multiple alignments of the *G. lateralis* amino acid sequences with those of orthologs from other arthropod species identified conserved domains and motifs essential for protein functions. Gl-Nvd had the Rieske domain and non-heme iron-binding motif characteristic of Rieske oxygenases (Suppl. Fig. 1). Gl-Phm, Gl-Dib, Gl-Sad, Gl-Spo, and Gl-CYP18a1 had a heme-binding domain with a PFxxGxRxCxG/A consensus sequence and conserved sequences in Helix-C (GxxWxEQRR), Helix-I (GxE/DTT/S), Helix-K (ExLR), and PERF motif (PxxFxPE/DRF) that are characteristic of cytochrome P450 enzymes (Suppl. Figs. 2–5, 8). In addition, Gl-Phm and Gl-Spo had the P/G-rich motif characteristic of the CYP2 clan (Suppl. Figs. 2, 3). Gl-NADK had the diacylglycerol kinase catalytic domain containing the GGDG motif, NE/D motif, and conserved domain II characteristic of NADKs (Suppl. Fig. 6). Gl-ALAS contained the 5-aminolevulinate synthase presequence and 5-aminolevulinate synthase catalytic domains characteristic of these enzymes in other species (Suppl. Fig. 7).

Table 2
Ecdysteroid metabolism contig sequences from the *G. lateralis* MLA YO transcriptome (Das et al., 2018). All contigs encoded full-length proteins. Abbreviations: aa, amino acids; bp, base pairs; and ORF, open reading frame.

Gene	Contig Number	GenBank Accession #	Contig Length (bp)	ORF (aa)
Phantom	c268220_g1_i1	OP555907	3513	564
Disembodied	c268194_g1_i1	OP555908	2452	538
Spook	c262802_g1_i1	OP555906	3241	520
Neverland	c218937_g1_i1	OP555905	1961	515
CYP18a1	c259236_g1_i1	OP555910	1845	527
Shadow	c247804_g1_i2	OP555909	2980	556
ALAS	c209048_g2_i2	OP572284	2696	532
NADK	c242467_g1_i5	OP722285	2109	452

Phylogenetic analysis confirmed the gene identities. Gl-Nvd, Gl-Phm, Gl-Spo, Gl-Sad, Gl-Dib, Gl-NADK, and Gl-ALAS clustered with their corresponding orthologs in other species (Fig. 1). Moreover, the cytochrome P450 enzymes in the CYP2 (Gl-Phm and Gl-Spo) and mitochondrion (Gl-Sad and Gl-Dib) clans formed two large groupings (Fig. 1).

3.2. Tissue expression of Gl-Phm, Gl-Spo, Gl-NADK, and Gl-ALAS

The mRNA levels of *Gl-Phm*, *Gl-Spo*, *Gl-NADK*, and *Gl-ALAS* were quantified in 10 tissues from intermolt *G. lateralis*. *Gl-Phm* and *Gl-Spo* were expressed in all tissues, but the mRNA levels were four orders of magnitude higher in the YO than the levels in the other nine tissues (Fig. 2A, B). By contrast, *Gl-ALAS* and *Gl-NADK* mRNA levels were similar in all ten tissues (Fig. 2C, D).

3.3. The effects of molt induction on YO gene expression

The effects of molt stage were determined in animals induced to molt by MLA. YOs were collected at different stages as determined by the R-index (Yu et al., 2002): intermolt (R = 7–9); early premolt (R = 11–13); mid-premolt (R = 16–18); and late premolt (R > 19). YOs were also collected from postmolt animals (10 days post-ecdysis). Hemolymph ecdysteroid level increased through premolt and was lowest in postmolt (Fig. 3). *Gl-Nvd*, *Gl-Spo*, *Gl-Phm*, and *Gl-CYP18a1* mRNA levels were higher during intermolt and premolt with the means at intermolt and premolt stages significantly higher than the means at postmolt (Fig. 4). *Gl-Sad* mRNA level was higher at mid-premolt and late premolt with the mean at mid-premolt significantly higher than the means at intermolt and postmolt (Fig. 4). By contrast, molt stage had no significant effect on *Gl-Dib* mRNA level and only limited effects on *Gl-NADK* and *Gl-ALAS* mRNA levels (Fig. 4). The mRNA levels were lowest at postmolt, with the means of *Gl-NADK* at intermolt and of *Gl-ALAS* at intermolt and early premolt significantly higher than the means at postmolt (Fig. 4).

The effects of molt induction by ESA on gene expression were determined. Intermolt animals were eyestalk ablated at Day 0. YOs were harvested from intact intermolt animals and from animals at 1, 3, 7, and 14 days post-ESA. There was a significant increase in hemolymph ecdysteroid titer, starting at 1 day post-ESA (Fig. 5A). ESA had no significant effect on *Gl-Nvd* mRNA level (Fig. 5B). *Gl-Spo* and *Gl-Phm* mRNA levels were lower at 3 days post-ESA than at 1 day post-ESA (Fig. 5C, 5F). *Gl-NADK*, *Gl-ALAS*, *Gl-Dib*, *Gl-Sad*, and *Gl-CYP18a1* mRNA levels significantly decreased by 14 days post-ESA (Fig. 5D, E, G, H, and I).

4. Discussion

Five genes in the ecdysteroid biosynthetic pathway and a 26-hydroxylase (*Cyp18a1*) were extracted from a *G. lateralis* YO transcriptome. Nvd plays a key role in ecdysteroid synthesis, as it converts cholesterol transported from the hemolymph to 7DC (Yoshiyama-Yanagawa et al., 2011). Gl-Nvd has the conserved regions characteristic of Rieske domain proteins (Sathapondecha et al., 2017; Yoshiyama-Yanagawa et al., 2011). Reductases and cytochrome P450 enzymes encoded by *Spo*, *Phm*, *Dib*, and *Sad* convert 7DC to ecdysone (Mykles, 2011). However, the YO can secrete other products in addition to ecdysone, depending on species and molt stage: 3-dehydroecdysone, 25-deoxyecdysone, and 3-dehydro-25-deoxyecdysone (Mykles, 2011). 20-Monooxygenases (Cyp314a1)

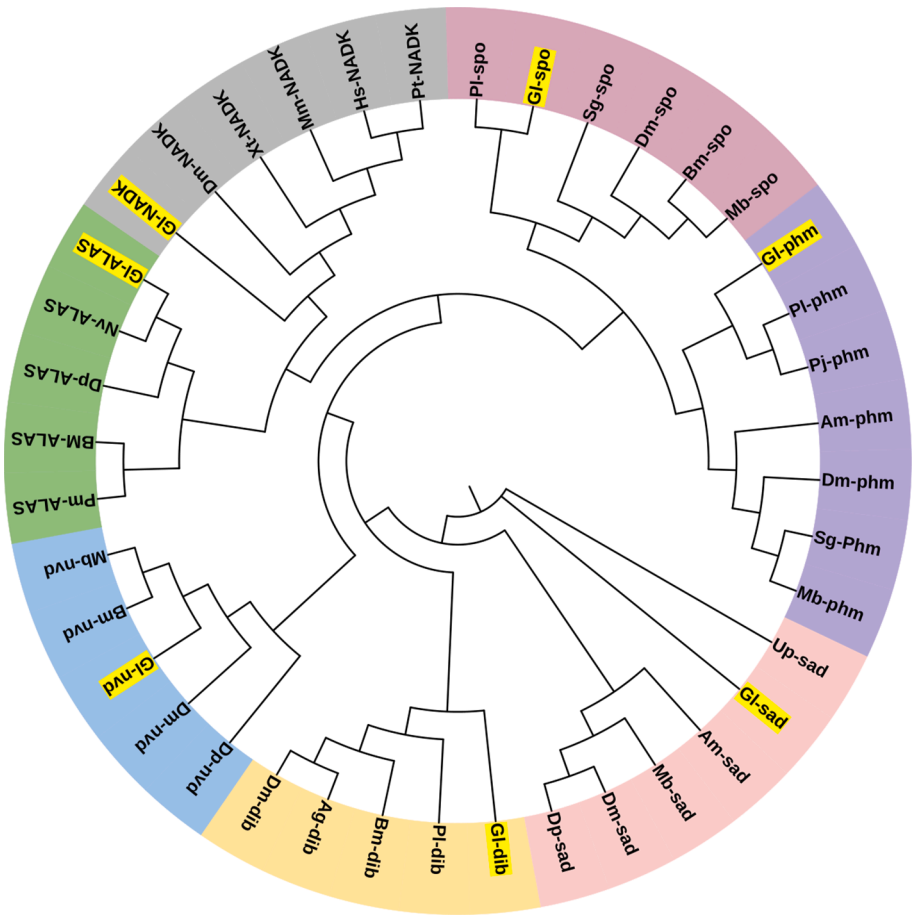

Fig. 1. Phylogenetic analysis of *G. lateralis* Neverland, Phantom, Disembodied, Spook, Shadow, NADK, and ALAS protein sequences. Abbreviations for crustacean species: Cm, *Carcinus maenas*; Dm', *Daphnia magna*; Es, *Eriocheir sinensis*; Ls, *Lepeophtheirus salmonis*; Pj, *Penaeus japonicus*; Pl, *Pontastacus leptodactylus*; Sp, *Scylla paramamosain*; and Up, *Uca pugilator*. Abbreviations for insect species: Ag, *Anopheles gambiae*; Am, *Apis mellifera*; Bd, *Bactrocera dorsalis*; Bm, *Bombyx mori*; Dm, *Drosophila melanogaster*; Dp, *Drosophila pachea*; Mb, *Mamestra brassicae*; Ms, *Manduca sexta*; Nv, *Nicrophorus vespilloide*; Pm, *Papilio machaon*; and Sg, *Schistocerca gregaria*. Abbreviations for vertebrate species: Hs, *Homo sapiens*; Mm, *Mus musculus*; Pt, *Pan troglodytes*; and Xt, *Xenopus tropicalis*. GenBank accession numbers of all sequences used for the analysis are given in Supplementary Data 2.

encoded by *Shed* in crustaceans and *Shade* in insects, hydroxylate ecdysteroid precursors at C20 to active products, such 20E and PA (Mykles, 2011; Swall et al., 2021; Ventura et al., 2017). Six *Shed* genes are expressed in the *G. lateralis* YO and other tissues (Swall et al., 2021). The *G. lateralis* Halloween enzymes and Cyp18a1 have all the conserved domains and motifs characteristic of cytochrome P450 proteins, with Gl-Spo and Gl-Phm assigned to the CYP2 clan and Gl-Dib, Gl-Sad, Gl-Shed, and Gl-Cyp18a1 assigned to the mitochondrial clan (Suppl. Fig. 2–5, 8) (Mykles, 2011; Swall et al., 2021). The mRNA levels of *Gl-Spo* and *Gl-Phm* were four orders of magnitude higher in the YO than their levels in nine other tissues (Fig. 2A, B). In other decapod species, Halloween genes (e.g. *Nvd*, *Spo*, and/or *Phm*) are highly expressed in the YO (Asazuma et al., 2009; Legrand et al., 2021; Sathapondecha et al., 2017). These data support the paradigm that the YO is the primary site for ecdysteroid synthesis. The gonad is also a site of ecdysteroidogenesis and expression of Halloween genes (Liu et al., 2021; Pan et al., 2022; Yuan et al., 2021a,b; 2022).

YO is also a site for 20E production, as *in vitro* assays show that the YO secretes both ecdysone and 20E (Swall et al., 2021). Unlike *Gl-Spo* and *Gl-Phm*, *Gl-Shed* mRNA levels in the YO are comparable to the levels in other tissues in intermolt animals (Swall et al., 2021). This suggests that peripheral tissues, which constitute a larger proportion of the body mass, such as skeletal muscle and the hepatopancreas, contribute more to total 20E and PA production than the YOs (Mykles, 2011). Thus, the general paradigm that the molting glands synthesize and secrete ecdysteroid precursors, which are converted to active hormones by peripheral tissues is consistent between insects and crustaceans (Gilbert and Rewitz, 2009; Mykles, 2011; Niwa and Niwa, 2014). However, *Gl-Shed5A* expression in the YO is higher than the other five *Gl-Sheds* and its mRNA level is increased in early premolt and mid-premolt animals (Swall et al., 2021), which suggests that the YO contributes to the increase in hemolymph 20E titers during premolt (Mykles, 2011; Mykles and Chang, 2020).

Cyp18a1 is a 26-hydroxylase that inactivates 20E and PA (Lafont et al., 2012; Mykles, 2011). It is expressed in a wide variety of tissues, including the YO and prothoracic gland of crustaceans and insects, respectively (Figs. 4, 5I) (Guittard et al., 2011; Mykles, 2011). In *Drosophila melanogaster*, Cyp18a1 is responsible for the decrease in 20E at the prepupal to pupal transition (Rewitz et al., 2010). Both ectopic overexpression and knockdown/knockout of *Cyp181a* in the prothoracic gland and other tissues disrupt development and result in third instar larval or pupal lethality (Guittard et al., 2011). These data indicate that Cyp18a1 contributes to the control of 20E levels around the time of metamorphosis. In MLA animals, *Gl-Cyp18a1* mRNA level is high at intermolt and is lower during premolt (Fig. 4). Assuming that *Gl-Cyp18a1* mRNA level serves as a proxy for Gl-Cyp18a1 protein and/or activity, this suggests that Gl-Cyp18a1 contributes to the secretion of 20E and other active ecdysteroids by the YO. Higher 26-hydroxylase activity during intermolt may contribute to the low ecdysteroid secretion by the basal YO, while lower 26-hydroxylase activity during premolt may contribute to higher ecdysteroid secretion by the activated and committed YO (Mykles, 2011; Mykles and Chang, 2020). Gl-Cyp18a1 may have a limited role during postmolt, when ecdysteroid synthesis and *Gl-Cyp18a1* mRNA level in the repressed YO are lowest (Fig. 4) (Mykles, 2011; Mykles and Chang, 2020). The repressed YO is transcriptionally quiescent, as mRNA levels of many genes are at their lowest (Das et al., 2018).

NADK and ALAS support ecdysteroidogenesis in the insect prothoracic gland. In *Bombyx mori*, *NADK* (*Bmb018637*) and *ALAS* (*Bmb021395*) are expressed in the prothoracic gland at more than ten times the level in brain (Nakaoka et al., 2017). In *D. melanogaster*, *NADK* (*CG33156*) and *ALAS* (*CG3017*) are preferentially expressed in the ring

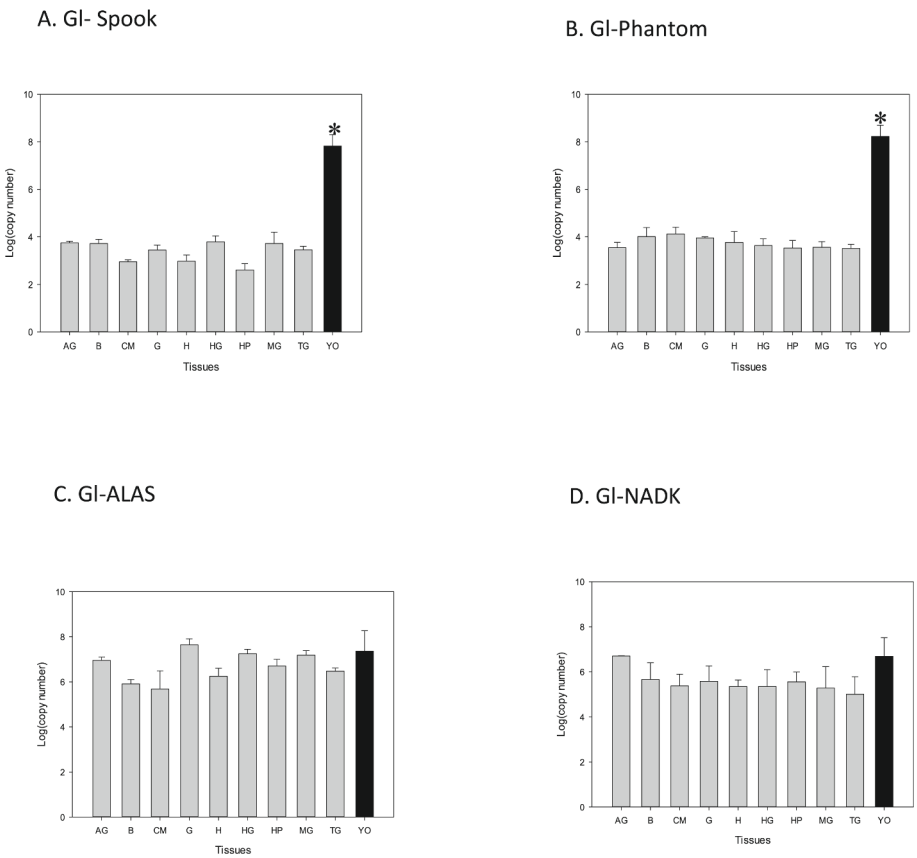

Fig. 2. Tissue distribution of *Gl-Spo*, *Gl-Phm*, *Gl-ALAS*, and *Gl-NADK* transcripts in intermolt *G. lateralis*. Abbreviations: AG, antennal gland; B, brain; CM, claw muscle; G, gill; H, heart; HG, hindgut; HP, hepatopancreas; MG, midgut; TG, thoracic ganglion; and YO, Y-organ. mRNA levels were quantified by qPCR. Data are presented as mean ± S.E.M. $\log_{10}$ copy number per μg total RNA (n = 3 for AG, HG, MG, and YO; n = 4 for G and HP; n = 5 for B, CM, and TG; n = 6 for H). Asterisks (Fig. 2A, B) indicate the means of *Gl-Spo* and *Gl-Phm* in the YO are significantly higher than the means in the other 9 tissues ($P < 0.001$).

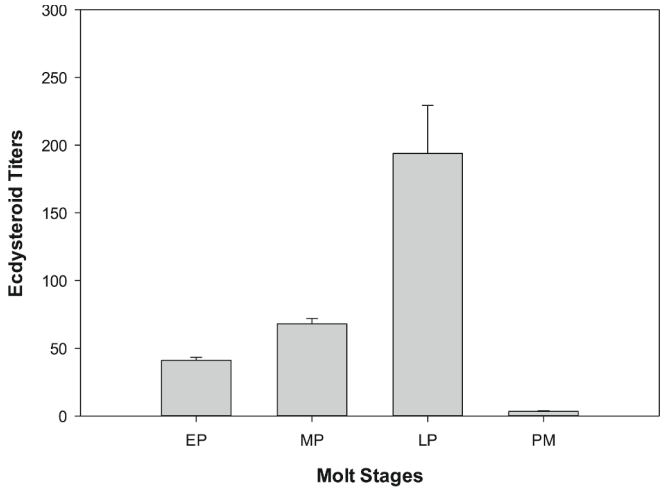

Fig. 3. Hemolymph ecdysteroid titers in *G. lateralis* induced to molt by MLA. Molt stages: early premolt (EP; stage D_0), mid-premolt (MP; stage D_1), late premolt (LP; stage $D_{2\text{-}3}$) and 10 days postmolt (PM). Data presented as mean ± S.E.M. pg 20E equivalents per μl hemolymph (EP, n = 6; MP, n = 8; LP, n = 10; and PM, n = 10). All means are significantly different from each other ($P < 0.05$).

gland and RNAi knockdown of either gene in the ring gland reduces whole-body 20E and makisterone A to basal levels (Nakaoka et al., 2017). ALAS is a pyridoxal phosphate-dependent enzyme that catalyzes the first step in heme biosynthesis (de Mena et al., 1999; Okano et al., 2010). NADK controls NADP production by phosphorylating NAD to NADP (Lerner et al., 2001; Love et al., 2015; Ohashi et al., 2012). Cytochrome P450 CYP monooxygenases (e.g., Spo, Phm, Dib, Sad, Shd/Shed, and Cyp18a1) require a heme cofactor for electron transfer and NADP(H) as an electron donor (Lafont et al., 2012; Nakaoka et al., 2017). As heme and NADP(H) are required for redox reactions in the cell, it is not surprising that *ALAS* and *NADK* are expressed in all *D. melanogaster* and *G. lateralis* tissues (Nakaoka et al., 2017)(Fig. 2C,D). However, unlike *D. melanogaster* and *B. mori*, *Gl-ALAS* and *Gl-NADK* were not preferentially expressed in the YO (Fig. 2C,D). Moreover, *Gl-ALAS* and *Gl-NADK* mRNA levels were higher in YOs from intermolt and premolt animals and lower in YO from postmolt animals (Fig. 4). This suggests that the mRNA levels are sufficient to support increased ecdysteroid production during premolt. Alternatively, NADP(H) can be provided by transaldolase, an enzyme in the pentose phosphate pathway. In *C. maenas* YO, transaldolase protein and activity are correlated with ecdysteroid synthesis, and transaldolase activity is inhibited by MIH (Lachaise et al., 1996). In *G. lateralis* YO, relative expression of transaldolase is increased by ESA (Shyamal et al., 2018).

Molting can be readily induced in *G. lateralis* by MLA and ESA. Animals can regenerate lost appendages, but they must molt to restore a functional limb (Bliss, 1979; Das, 2015). Autotomy of five to eight walking legs causes precocious molts in order to regain mobility as quickly as possible (Skinner, 1985; Yu et al., 2002). Impaired mobility from MLA is especially serious for a terrestrial species, such as *G. lateralis*, which lack the neutral buoyancy of water to support the body (Mykles and Chang, 2020). MLA produces physiological changes consistent with natural molts. *G. lateralis* enter premolt three to six weeks after MLA, complete premolt in about three weeks, molt successfully, and complete postmolt in three to four weeks (Mykles, 2001; Pitts et al., 2017; Skinner, 1985; Skinner and Graham, 1970; Yu et al., 2002). By contrast, ESA induces molting by the acute withdrawal of MIH, and animals enter premolt by 1 day post-ESA (Bliss, 1979; Mykles and Chang, 2020). Although it is an effective experimental technique to synchronize animals to a molt stimulus, ESA also causes reductions of other neuropeptides that control critical physiological processes, such as

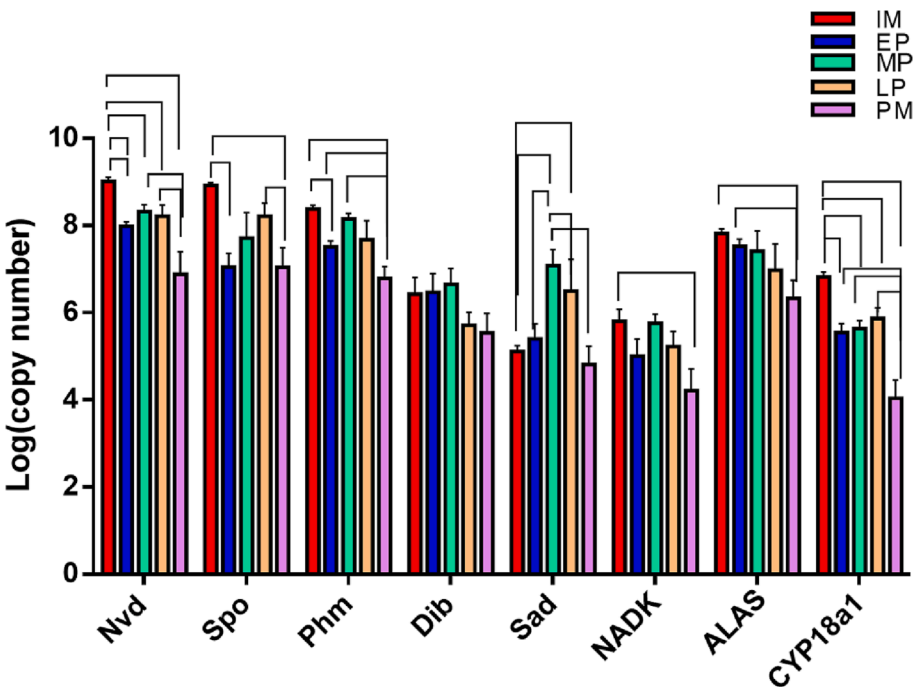

Fig. 4. Expression of *Gl-ALAS*, *Gl-CYP18A1*, *Gl-Dib*, *Gl-NADK*, *Gl-Nvd*, *Gl-Phm*, *Gl-Sad*, and *Gl-Spo* in the YO of *G. lateralis* induced to molt by MLA. mRNA levels at intermolt (IM; stage C_4); early premolt (EP; stage D_0), mid-premolt (MP; stage D_1), late premolt (LP; stage D_2) and 10 days postmolt (PM) were quantified by qPCR. Data are presented as mean ± S.E.M $\log_{10}$ copy number per μg total RNA (IM, n = 10; EP, n = 6; MP, n = 8; LP, n = 10; and PM, n = 10). Brackets indicate means that are significantly different from each other ($P < 0.05$).

glucose metabolism, reproduction, development, immunity, and ion and water balance (Chen et al., 2020). Animals proceed through premolt, but fail to molt successfully, which likely results from the disruption of hormonal control (Skinner, 1985). Nonetheless, it is still informative to compare the effects of MLA and ESA on gene expression. Similar responses may indicate a common mechanism, whereas different responses may not be directly attributed to molting, particularly after prolonged withdrawal of eyestalk neuropeptides in mid-premolt animals by 14 days post-ESA. The significant drop of *Gl-ALAS*, *Gl-NADK*, *Gl-Dib*, and *Gl-Sad* mRNA levels in the YO at 14 days post-ESA may have resulted from dysregulation of organ systems maintaining organismal homeostasis (Fig. 5D, E, G, and H).

The effects of molt stage on Halloween gene expression in the YO vary between species and individual genes. In *C. sapidus*, mRNA levels of *Cs-Spo* and *Cs-Nvd* were quantified in the YOs from animals at intermolt, early premolt, and mid-premolt stages (Legrand et al., 2021). Although *Cs-Spo* and *Cs-Nvd* mRNA levels were higher at premolt stages than at intermolt, only the *Cs-Nvd* means between intermolt and early premolt were significantly different (Legrand et al., 2021). In *M. japonicas*, *Mj-Phm* mRNA level is 7-fold higher at premolt than at intermolt (Asazuma et al., 2009). Moreover, rMIH and sinus gland extract decrease *Mj-Phm* mRNA level in activated YOs after 24 h in an *in vitro* assay (Asazuma et al., 2009). In *P. monodon*, *Pm-Nvd* mRNA level in the YO increases only ~4-fold in mid-premolt (stage D_1) compared to intermolt (stage C) animals (Sathapondecha et al., 2017). RNAi knockdown of *Pm-Nvd* decreases hemolymph 20E titer and delays molting (Sathapondecha et al., 2017). In *Macrobrachium nipponense*, *Mn-Phm* is highly expressed in ovary and testis, but *Mn-Phm* mRNA level in the YO was not examined (Pan et al., 2022). However, RNAi knockdown of *Mn-Phm* decreases 20E content and molting frequency (Pan et al., 2022). In *G. lateralis*, the expression of five Halloween genes was quantified in the YO at five molt stages. *Gl-Nvd*, *Gl-Spo,* and *Gl-Phm* showed a similar expression pattern, with highest mRNA levels at intermolt, lowest levels at postmolt, and intermediate levels at premolt stages (Fig. 4). *Gl-Dib* mRNA level was not affected by molt stage. Only *Gl-Sad* showed an expression pattern consistent with YO ecdysteroid synthesis, with the highest mRNA levels at mid- and late premolt (stages D_1 and D_2; Fig. 4).

ESA is an effective method to induce molting in most decapod species (Skinner, 1985). As the X-organ/sinus gland complex is the primary source of MIH, ESA results in YO activation and increases in hemolymph ecdysteroid titers (Fig. 5A). However, some species, such as green shore crab (*C. maenas*), are refractory to ESA (Abuhagr et al., 2014a). The effects of ESA on hemolymph ecdysteroid titer and YO gene expression vary between species and between different Halloween genes, so that ecdysteroid titer and mRNA levels are not always correlated. In *Portunus trituberculatus*, mRNA levels of *Pt-Dib* and *Pt-Sad* are transiently increased, reaching maximum levels at 4 days post-ESA, while *Pt-Spo* mRNA level is unchanged (Xie et al., 2016). *P. trituberculatus* appears to be refractory to ESA, as hemolymph titer increased no more than two-fold by 4 days post-ESA (Xie et al., 2016). In *C. sapidus*, hemolymph ecdysteroid titer and YO mRNA levels of *Cs-Nvd*, *Cs-Spo*, *Cs-Dib*, and *Cs-Sad* increase in early premolt animals induced by ESA (Legrand et al., 2021). By contrast, in *G. lateralis*, ESA had no or only transitory effects on the mRNA levels of *Gl-Nvd*, *Gl-Spo*. *Gl-Phm*, *Gl-Dib*, and *Gl-Sad* between 0 and 7 days post-ESA; the levels were not correlated with hemolymph 20E titers (Fig. 5; compare A with B, C, F, G, and H). The results from qPCR conflict with those from RNA-seq data reported by Shyamal et al. (2018). ESA increased relative expression of *Gl-Nvd*, *Gl-Spo*, *Gl-Phm*, *Gl-Dib*, and *Gl-Sad* (see Suppl. Fig, 5G in Shyamal et al., 2018). This illustrates that RNA-seq data should be interpreted with caution when a low number of biological replicates (n = 3) are used. A standard practice is to confirm RNA-seq data with qPCR quantification (e.g., see Legrand et al., 2021).

Molting gland ecdysteroidogenesis is mediated by mTORC1 in both insects and crustaceans (Mykles, 2021). mTORC1 controls the global translation of mRNA into protein in eukaryotic cells (Battaglioni et al., 2022; Melick and Jewell, 2020; Saxton and Sabatini, 2017). In insects, mTORC1 inactivation blocks prothoracicotropic hormone- and growth factor-stimulated increases in ecdysteroid synthesis by the prothoracic gland (Gu et al., 2012; Kemirembe et al., 2012; Rewitz et al., 2013; Scieuzo et al., 2018; Smith and Rybczynski, 2012; Teleman, 2010). YO activation in early premolt (stage D_0) requires mTORC1-dependent protein synthesis (Mykles, 2021). Rapamycin inhibits YO ecdysteroidogenesis *in vitro* and inhibits YO activation *in vivo* (Abuhagr et al., 2014b, 2016; Shyamal et al., 2018). Later in the early premolt stage, mTORC1 activity controls, either directly or indirectly, the expression of thousands of genes (Shyamal et al., 2018). Most notably, mTORC1 and TGFβ/Activin/Myostatin (Mstn) signaling pathway genes are up-

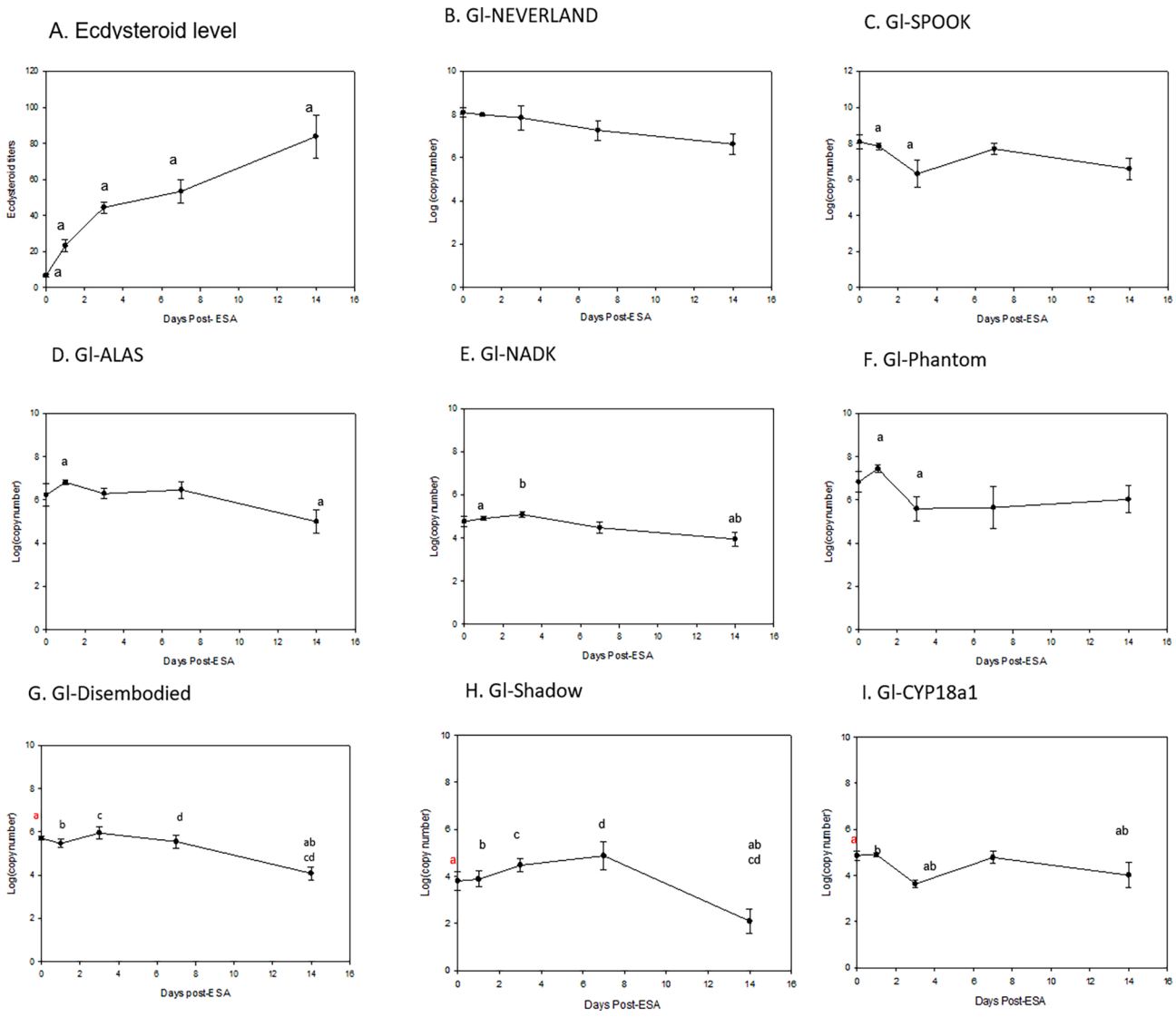

Fig. 5. Effects of molt induction by ESA on hemolymph ecdysteroid titer (A) and gene expression in *G. lateralis* YO (B-I). Hemolymph and YOs tissues collected from intact (Day 0) animals and from animals 1 day, 3 days, 7 days, or 14 days post-ESA. Ecdysteroid levels were quantified by ELISA and data presented as mean ± S.E.M. pg 20E equivalents per µl hemolymph. mRNA levels were quantified by qPCR and data are presented as mean ± S.E.M $\log_{10}$ copy number per µg total RNA. Samples sizes (n) were 8 for Day 0, 6 for Day 1, 8 for Day 3, 8 for Day 7, and 7 for Day 14. Means designated by the same letter are significantly different from each other ($P < 0.05$).

regulated and MIH signaling pathway genes are down-regulated in *G. lateralis* induced to molt by MLA and ESA (Abuhagr et al., 2014b; Das et al., 2018; Mykles, 2021; Shyamal et al., 2018). In *G. lateralis*, *C. sapidus*, and *Metacarcinus magister*, YO *Rheb* expression is increased during premolt, indicating that *Rheb* mRNA level can serve as a marker for mTORC1-dependent ecdysteroidogenesis (Abuhagr et al., 2014b; Roegner and Watson, 2020; Wittmann et al., 2018). TGF β /Activin/ Mstn signaling mediates the transition of the YO to the committed state in mid-premolt, as *Gl-Mstn* mRNA level peaks at 3 days post-ESA and SB431542, an inhibitor of Activin receptor signaling, prevents *G. lateralis* from transitioning from early premolt to mid-premolt (Abuhagr et al., 2016). By contrast, mRNA levels of ecdysteroid synthetic enzymes are not consistently higher during premolt or not correlated with hemoymph ecdysteroid titers (Figs. 4, 5) (Asazuma et al., 2009; Legrand et al., 2021; Sathapondecha et al., 2017; Xie et al., 2016). These data suggest that the regulation of ecdysteroidogenic enzymes during the intermolt and premolt stages is primarily at the translational level by mTORC1.

5. Conclusions

The YO is the major site of ecdysteroid synthesis in decapod crustaceans. Contigs extracted from *G. lateralis* YO transcriptomes encode five Halloween enzymes (*Gl-Nvd*, *Gl-Spo*, *Gl-Phm*, *Gl-Dib*, and *Gl-Sad*), two enzymes that may support ecdysteroid synthesis (*Gl-NADK* and *Gl-ALAS*), and one enzyme that inactivates 20E and PA (*Gl-Cyp18a1*). To our knowledge, this is the first study comparing the effects of two molt induction methods on the expression of five Halloween genes in the YO. Acute withdrawal of MIH and other eyestalk neuropeptides by ESA had little or no consistent effect on mRNA levels 0 to 7 days post-ESA and those levels were not correlated with hemolymph ecdysteroid titer. In animals induced to molt by MLA, only *Gl-Sad* mRNA level was correlated with high YO ecdysteroidogenesis in mid- and late premolt. By contrast, the mRNA levels of the other four Halloween genes were higher in intermolt animals. These data suggest that the increased ecdysteroidogenic capacity in the *G. lateralis* YO is primarily driven by mTORC1-mediated translation of mRNA to protein. Thus, the basal YO is primed to respond rapidly to the drop in hemolymph MIH titer and

initiate molting. The up-regulation of *Gl-Sad*, which hydroxylates C2 to form ecdysone, may sustain the high rates of ecdysteroid synthesis by the committed YO. The mRNA levels of Halloween genes, except for *Sad*, may be unreliable markers for YO ecdysteroid activity in *G. lateralis*.

CRediT authorship contribution statement

Samiha A.M. Benrabaa: Conceptualization, Visualization, Investigation, Writing – original draft, Writing – review & editing. **Sharon A. Chang:** ELISA data acquisition. **Ernest S. Chang:** ELISA data analysis, Writing - review & editing. **Donald L. Mykles:** Supervision, Conceptualization, Funding acquisition, Writing – review & editing.

Declaration of Competing Interest

The authors declare that they have no known competing financial interests or personal relationships that could have appeared to influence the work reported in this paper.

Data availability

Data will be made available on request.

Acknowledgements

This research was supported by grants from the National Science Foundation (IOS-1257732 and IOS-1922701). We thank Hector C. Horta and Rafael Polanco for collecting *G. lateralis* and the Ministry of Environment and Natural Resources of the Dominican Republic under Contract for Access to Genetic Resources for Research Purposes DJC-1-2019-01310 and Collection and Export Permit No. VAPS-07979.

Appendix A. Supplementary data

Supplementary data to this article can be found online at https://doi.org/10.1016/j.ygcen.2023.114304.

References

Abuhagr, A.M., Blindert, J.L., Nimitkul, S., Zander, I.A., LaBere, S.M., Chang, S.A., MacLea, K.S., Chang, E.S., Mykles, D.L., 2014a. Molt regulation in green and red color morphs of the crab *Carcinus maenas*: gene expression of molt-inhibiting hormone signaling components. J. Exp. Biol. 217, 796–808.

Abuhagr, A.M., MacLea, K.S., Chang, E.S., Mykles, D.L., 2014b. Mechanistic target of rapamycin (mTOR) signaling genes in decapod crustaceans: Cloning and tissue expression of mTOR, Akt, Rheb, and p70 S6 kinase in the green crab, *Carcinus maenas*, and blackback land crab, *Gecarcinus lateralis*. Comp. Biochem. Physiol. 168A, 25–39.

Abuhagr, A.M., MacLea, K.S., Mudron, M.R., Chang, S.A., Chang, E.S., Mykles, D.L., 2016. Roles of mechanistic target of rapamycin and transforming growth factor-beta signaling in the molting gland (Y-organ) of the blackback land crab, *Gecarcinus lateralis*. Comp. Biochem. Physiol. 198A, 15–21.

Andersen, Ø., Johnsen, H., Wittmann, A.C., Harms, L., Thesslund, T., Berg, R.S., Siikavuopio, S., Mykles, D.L., 2022. *De novo* transcriptome assemblies of red king crab (*Paralithodes camtschaticus*) and snow crab (*Chionoecetes opilio*) molting gland and eyestalk ganglia - Temperature effects on expression of molting and growth regulatory genes in adult red king crab. Comp. Biochem. Physiol. 257B, 110678.

Artimo, P., Jonnalagedda, M., Arnold, K., Baratin, D., Csardi, G., de Castro, E., Duvaud, S., Flegel, V., Fortier, A., Gasteiger, E., Grosdidier, A., Hernandez, C., Ioannidis, V., Kuznetsov, D., Liechti, R., Moretti, S., Mostaguir, K., Redaschi, N., Rossier, G., Xenarios, I., Stockinger, H., 2012. ExPASy: SIB bioinformatics resource portal. Nucl. Acids Res. 40 (W1), W597–W603.

Asazuma, H., Nagata, S., Nagasawa, H., 2009. Inhibitory effect of molt-inhibiting hormone on *Phantom* expression in the Y-organ of the kuruma prawn, *Marsupenaeus japonicus*. Arch. Insect Biochem. Physiol. 72, 220–233.

Battaglioni, S., Benjamin, D., Wälchli, M., Maier, T., Hall, M.N., 2022. mTOR substrate phosphorylation in growth control. Cell 185, 1814–1836.

Bliss, D.E., 1979. From sea to tree – Saga of a land crab. Am. Zool. 19, 385–410.

Chen, H.Y., Toullec, J.Y., Lee, C.Y., 2020. The crustacean hyperglycemic hormone superfamily: progress made in the past decade. Front. Endocrinol. 11, 578958.

Covi, J.A., Chang, E.S., Mykles, D.L., 2009. Conserved role of cyclic nucleotides in the regulation of ecdysteroidogenesis by the crustacean molting gland. Comp. Biochem. Physiol. 152, 470–477.

Das, S., 2015. Morphological, molecular, and hormonal basis of limb regeneration across Pancrustacea. Integr. Comp. Biol. 55, 869–877.

Das, S., Vraspir, L., Zhou, W., Durica, D.S., Mykles, D.L., 2018. Transcriptomic analysis of differentially expressed genes in the molting gland (Y-organ) of the blackback land crab, *Gecarcinus lateralis*, during molt-cycle stage transitions. Comp. Biochem. Physiol. 28D, 37–53.

de Mena, I.R., Fernandez-Moreno, M.A., Bornstein, B., Kaguni, L.S., Garesse, R., 1999. Structure and regulated expression of the delta-aminolevulinate synthase gene from *Drosophila melanogaster*. J. Biol. Chem. 274, 37321–37328.

Dermauw, W., Van Leeuwen, T., Feyereisen, R., 2020. Diversity and evolution of the P450 family in arthropods. Insect Biochem. Molec. Biol. 127, 103490.

Feyereisen, R., 2012. Insect CYP Genes and P450 Enzymes. In: Gilbert, L.I. (Ed.), Insect Molecular Biology and Biochemistry. Academic Press, New York, pp. 236–316.

Gilbert, L.I., Rewitz, K.F., 2009. The function and evolution of the halloween genes: The pathway to the arthropod molting hormone. In: Smagghe, G. (Ed.), Ecdysone: Structures and Function. Springer, Netherlands, pp. 231–269.

Gu, S.-H., Yeh, W.-L., Young, S.-C., Lin, P.-L., Li, S., 2012. TOR signaling is involved in PTTH-stimulated ecdysteroidogenesis by prothoracic glands in the silkworm, *Bombyx mori*. Insect Biochem. Molec. Biol. 42, 296–303.

Guittard, E., Blais, C., Maria, A., Parvy, J.-P., Pasricha, S., Lumb, C., Lafont, R., Daborn, P.J., Dauphin-Villemant, C., 2011. CYP18A1, a key enzyme of *Drosophila* steroid hormone inactivation, is essential for metamorphosis. Dev. Biol. 349, 35–45.

Hopkins, P.M., 2012. The eyes have it: a brief history of crustacean neuroendocrinology. Gen. Comp. Endocrinol. 175, 357–366.

Hou, X., Yang, H.e., Chen, X., Wang, J., Wang, C., 2021. RNA interference of mTOR gene delays molting process in *Eriocheir sinensis*. Comp. Biochem. Physiol. 256B, 110651.

Iga, M., Smagghe, G., 2010. Identification and expression profile of Halloween genes involved in ecdysteroid biosynthesis in *Spodoptera littoralis*. Peptides 31, 456–467.

Kamiyama, T., Niwa, R., 2022. Transcriptional regulators of ecdysteroid biosynthetic enzymes and their roles in insect development. Front. Physiol. 13, 823418.

Kannangara, J.R., Mirth, C.K., Warr, C.G., 2021. Regulation of ecdysone production in *Drosophila* by neuropeptides and peptide hormones. Open Biology 11, 200373.

Kemirembe, K., Liebmann, K., Bootes, A., Smith, W.A., Suzuki, Y., 2012. Amino acids and TOR signaling promote prothoracic gland growth and the initiation of larval molts in the tobacco hornworm *Manduca sexta*. PloS One 7, e44429.

Lachaise, F., Sommé, G., Carpentier, G., Granjeon, E., Webster, S., Baghdassarian, D., 1996. A transaldolase - An enzyme implicated in crab steroidogenesis. Endocrine 5, 23–32.

Lafont, R., Dauphin-Villemant, C., Warren, J.T., Rees, H., 2012. Ecdysteroid chemistry and biochemistry. In: Gilbert, L.I. (Ed.), Insect Endocrinology. Elsevier, San Diego, pp. 106–176.

Larkin, M.A., Blackshields, G., Brown, N.P., Chenna, R., McGettigan, P.A., McWilliam, H., Valentin, F., Wallace, I.M., Wilm, A., Lopez, R., Thompson, J.D., Gibson, T.J., Higgins, D.G., 2007. Clustal W and clustal X version 2.0. Bioinformatics 23, 2947-2948.

Legrand, E., Bachvaroff, T., Schock, T.B., Chung, J.S., 2021. Understanding molt control switches: Transcriptomic and expression analysis of the genes involved in ecdysteroidogenesis and cholesterol uptake pathways in the Y-organ of the blue crab, *Callinectes sapidus*. PloS One 16, e0256735.

Lerner, F., Niere, M., Ludwig, A., Ziegler, M., 2001. Structural and functional characterization of human NAD kinase. Biochem. Biophy. Res. Commun. 288, 69–74.

Letunic, I., Bork, P., 2016. Interactive tree of life (iTOL) v3: an online tool for the display and annotation of phylogenetic and other trees. Nucl. Acids Res. 44 (W1), W242–W245.

Liu, J., Zhou, T., Wang, C., Chan, S., Wang, W., 2021. Deciphering the molecular regulatory mechanism orchestrating ovary development of the Pacific whiteleg shrimp *Litopenaeus vannamei* through integrated transcriptomic analysis of reproduction-related organs. Aquaculture 533, 736160.

Love, N.R., Pollak, N., Dölle, C., Niere, M., Chen, Y., Oliveri, P., Amaya, E., Patel, S., Ziegler, M., 2015. NAD kinase controls animal NADP biosynthesis and is modulated via evolutionarily divergent calmodulin-dependent mechanisms. Proc. Natl. Acad. Sci. USA 112, 1386–1391.

Marchler-Bauer, A., Derbyshire, M.K., Gonzales, N.R., Lu, S.N., Chitsaz, F., Geer, L.Y., Geer, R.C., He, J., Gwadz, M., Hurwitz, D.I., Lanczycki, C.J., Lu, F., Marchler, G.H., Song, J.S., Thanki, N., Wang, Z.X., Yamashita, R.A., Zhang, D.C., Zheng, C.J., Bryant, S.H., 2015. CDD: NCBI's conserved domain database. Nucl. Acids Res. 43, D222–D226.

Melick, C.H., Jewell, J.L., 2020. Regulation of mTORC1 by upstream stimuli. Genes 11, 989.

Mykles, D.L., 2001. Interactions between limb regeneration and molting in decapod crustaceans. Am. Zool. 41, 399–406.

Mykles, D.L., 2011. Ecdysteroid metabolism in crustaceans. J. Steroid Biochem. Molec. Biol. 127, 196–203.

Mykles, D.L., 2021. Signaling pathways that regulate the crustacean molting gland. Front. Endocrinol. 12, 674711.

Mykles, D.L., Chang, E.S., 2020. Hormonal control of the crustacean molting gland: Insights from transcriptomics and proteomics. Gen. Comp. Endocrinol. 294, 113493.

Nakaoka, T., Iga, M., Yamada, T., Koujima, I., Takeshima, M., Zhou, X.Y., Suzuki, Y., Ogihara, M.H., Kataoka, H., 2017. Deep sequencing of the prothoracic gland transcriptome reveals new players in insect ecdysterodogenesis. PloS One 12, e0172951.

Nicholas, K.B., Nicholas, H.B., Deerfield, D., 1997. GeneDoc: analysis and visualization of genetic variation. EMBNEW News 4, 14.

Niwa, R., Niwa, Y.S., 2014. Enzymes for ecdysteroid biosynthesis: their biological functions in insects and beyond. Biosci. Biotechnol. Biochem. 78, 1283–1292.

Ohashi, K., Kawai, S., Murata, K., 2012. Identification and characterization of a human mitochondrial NAD kinase. Nature Commun. 3, 1248.
Okano, S., Zhou, L.Y., Kusaka, T., Shibata, K., Shimizu, K., Gao, X., Kikuchi, Y., Togashi, Y., Hosoya, T., Takahashi, S., Nakajima, O., Yamamoto, M., 2010. Indispensable function for embryogenesis, expression and regulation of the nonspecific form of the 5-aminolevulinate synthase gene in mouse. Genes Cells 15, 77–89.
Okonechnikov, K., Golosova, O., Fursov, M., UGENE Team, 2012. Unipro UGENE: a unified bioinformatics toolkit. Bioinformatics 28, 1166–1167.
Pan, X.Y., Connacher, R.P., O'Connor, M.B., 2021. Control of the insect metamorphic transition by ecdysteroid production and secretion. Curr. Opinion Insect Sci. 43, 11–20.
Pan, F., Fu, Y., Zhang, W., Jiang, S., Xiong, Y., Yan, Y., Gong, Y., Qiao, H., Fu, H., 2022. Characterization, expression and functional analysis of CYP306a1 in the oriental river prawn, *Macrobrachium nipponense*. Aquaculture Rep. 22, 101009.
Pitts, N.L., Schulz, H.M., Oatman, S.R., Mykles, D.L., 2017. Elevated expression of neuropeptide signaling genes in the eyestalk ganglia and Y-organ of *Gecarcinus lateralis* individuals that are refractory to molt induction. Comp. Biochem. Physiol. 214B, 66–78.
Rewitz, K.F., Yamanaka, N., O'Connor, M.B., 2013. Developmental checkpoints and feedback circuits time insect maturation, in: Y.B. Shi (Ed.), Animal Metamorphosis, 1-33.
Rewitz, K.F., Yamanaka, N., O'Connor, M.B., 2010. Steroid hormone inactivation is required during the juvenile-adult transition in *Drosophila*. Dev. Cell 19, 895–902.
Roegner, M.E., Watson, R.D., 2020. *De novo* transcriptome assembly and functional annotation for Y-organs of the blue crab (*Callinectes sapidus*), and analysis of differentially expressed genes during pre-molt. Gen. Comp. Endocrinol. 298, 113567.
Santiago-Sotelo, P., Ramirez-Prado, J.H., 2012. prfectBLAST: a platform-independent portable front end for the command terminal BLAST plus stand-alone suite. Biotechniques 53, 299–300.
Sathapondecha, P., Panyim, S., Udomkit, A., 2017. An essential role of Rieske domain oxygenase Neverland in the molting cycle of black tiger shrimp, *Penaeus monodon*. Comp. Biochem. Physiol. 213A, 11–19.
Saxton, R.A., Sabatini, D.M., 2017. mTOR signaling in growth, metabolism, and disease. Cell 168, 960–976.
Scieuzo, C., Nardiello, M., Salvia, R., Pezzi, M., Chicca, M., Leis, M., Bufo, S.A., Vinson, S. B., Rao, A., Vogel, H., Falabella, P., 2018. Ecdysteroidogenesis and development in *Heliothis virescens* (Lepidoptera: Noctuidae): Focus on PTTH-stimulated pathways. J. Insect Physiol. 107, 57–67.
Shyamal, S., Das, S., Guruacharya, A., Mykles, D.L., Durica, D.S., 2018. Transcriptomic analysis of crustacean molting gland (Y-organ) regulation via the mTOR signaling pathway. Sci. Rep. 8, 7307.
Skinner, D.M., 1985. Molting and regeneration. In: Bliss, D.E., Mantel, L.H. (Eds.), The Biology of Crustacea. Academic Press, New York, pp. 43–146.
Skinner, D.M., Graham, D.E., 1970. Molting in land crabs: stimulation by leg removal. Science 169, 383–385.
Smith, W., Rybczynski, R., 2012. Prothoracicotropic hormone. In: Gilbert, L.I. (Ed.), Insect Endocrinology. Elsevier, San Diego, pp. 1–62.
Swall, M.E., Benrabaa, S.A.M., Tran, N.M., Tran, T.D., Ventura, T., Mykles, D.L., 2021. Characterization of Shed genes encoding ecdysone 20-monooxygenase (CYP314A1) in the Y-organ of the blackback land crab, *Gecarcinus lateralis*. Gen. Comp. Endocrinol. 301, 113658.
Teleman, A.A., 2010. Molecular mechanisms of metabolic regulation by insulin in *Drosophila*. Biochem. J. 425, 13–26.
Thompson, J.D., Higgins, D.G., Gibson, T.J., 1994. Clustal W – improving the sensitivity of progressive multiple sequence alignment through sequence weighting, position-specific gap penalties, and weight matrix choice. Nucl. Acids Res. 22, 4673–4680.
Tom, M., Manfrin, C., Giulianini, P.G., Pallavicini, A., 2013. Crustacean oxi-reductases protein sequences derived from a functional genomic project potentially involved in ecdysteroid hormones metabolism – a starting point for function examination. Gen. Comp. Endocrinol. 194, 71–80.
Ventura, T., Bose, U., Fitzgibbon, Q.P., Smith, G.G., Shaw, P.N., Cummins, S.F., Elizur, A., 2017. CYP450s analysis across spiny lobster metamorphosis identifies a long sought missing link in crustacean development. J. Steroid Biochem. Molec. Biol. 171, 262–269.
Ventura, T., Palero, F., Rotllant, G., Fitzgibbon, Q.P., 2018. Crustacean metamorphosis: an omics perspective. Hydrobiologia 825, 47–60.
Wang, B., Yang, J.R., Gao, C.C., Hao, T., Li, J.J., Sun, J.S., 2020. Reconstruction of *Eriocheir sinensis* Y-organ genome-scale metabolic network and differential analysis after eyestalk ablation. Front. Genetics 11, 532492.
Wittmann, A.C., Benrabaa, S.A.M., Lopez-Ceron, D.A., Chang, E.S., Mykles, D.L., 2018. Effects of temperature on survival, moulting, and expression of neuropeptide and mTOR signalling genes in juvenile Dungeness crab (*Metacarcinus magister*). J. Exp. Biol. 221, jeb187492.
Xie, X., Liu, Z.Y., Liu, M.X., Tao, T., Shen, X.Q., Zhu, D.F., 2016. Role of Halloween genes in ecdysteroids biosynthesis of the swimming crab (*Portunus trituberculatus*): Implications from RNA interference and eyestalk ablation. Comp. Biochem. Physiol. 199A, 105–110.
Yoshiyama-Yanagawa, T., Enya, S., Shimada-Niwa, Y., Yaguchi, S., Haramoto, Y., Matsuya, T., Shiomi, K., Sasakura, Y., Takahashi, S., Asashima, M., Kataoka, H., Niwa, R., 2011. The conserved Rieske oxygenase DAF-36/Neverland is a novel cholesterol-metabolizing enzyme. J. Biol. Chem. 286, 25756–25762.
Yu, X., Chang, E.S., Mykles, D.L., 2002. Characterization of limb autotomy factor-proecdysis (LAF_{pro}), isolated from limb regenerates, that suspends molting in the land crab *Gecarcinus lateralis*. Biol. Bull. 202, 204–212.
Yuan, H., Qiao, H., Fu, Y., Fu, H., Zhang, W., Jin, S., Gong, Y., Jiang, S., Xiong, Y., Hu, Y., Wu, Y., 2021a. RNA interference shows that Spook, the precursor gene of 20-hydroxyecdysone (20E), regulates the molting of *Macrobrachium nipponense*. J. Steroid Biochem. Molec. Biol. 213, 105976.
Yuan, H.W., Zhang, W.Y., Fu, Y., Jiang, S.F., Xiong, Y.W., Zhai, S.H., Gong, Y.S., Qiao, H., Fu, H.T., Wu, Y., 2021b. MnFtz-f1 is required for molting and ovulation of the oriental river prawn *Macrobrachium nipponense*. Front. Endocrinol. 12, 798577.
Yuan, H.W., Zhang, W.Y., Qiao, H., Jin, S.B., Jiang, S.F., Xiong, Y.W., Gong, Y.S., Fu, H. T., 2022. MnHR4 functions during molting of *Macrobrachium nipponense* by regulating 20E synthesis and mediating 20E signaling. Int. J. Molec. Sci. 23, 12528.